Polymer 146 (2018) 222–229

Contents lists available at ScienceDirect

Polymer

journal homepage: www.elsevier.com/locate/polymer

Molecular influence in the glass/polymer interface design: The role of segmental dynamics

Alex J. Hsieh [a, b, *], David Veysset [b, c], Daniel F. Miranda [d], Steven E. Kooi [b], James Runt [d], Keith A. Nelson [b, c]

[a] U.S. Army Research Laboratory, RDRL-WMM-G, Aberdeen Proving Ground, MD, 21005-5069, USA
[b] Institute for Soldier Nanotechnologies, MIT, Cambridge, MA, 02139, USA
[c] Department of Chemistry, MIT, Cambridge, MA, 02139, USA
[d] Department of Materials Science and Engineering, Penn State University, University Park, PA, 16802, USA

ARTICLE INFO

Article history:
Received 5 February 2018
Received in revised form
5 May 2018
Accepted 9 May 2018
Available online 15 May 2018

Keywords:
Dynamic impedance
Shock Hugoniot
Segmental dynamics
Poly(urethane urea)
Polyurea
Glass/polymer interface
Dynamic stiffening
High-rate deformation-induced glass transition
Microballistics

ABSTRACT

Recent observations of the high-velocity impact response in poly (urethane urea), PUU, elastomers has inspired a new inquiry on whether enabling molecular mechanisms could benefit dynamic impedance optimization at the interface of a glass/polymer bilayer, particularly at the moment of impulse interaction. In this work, we investigate the molecular influence on dynamic impedance using microballistic measurements on two bulk elastomers, a PUU and a polyurea, PU. Upon impact at strain rates ~10^8/s, PUU exhibits a moderate improvement in resistance against penetration than PU, that is more pronounced at higher speeds. The variation in dynamic stiffening corroborates well with the corresponding segmental dynamics data determined via broadband dielectric relaxation. Meanwhile, we calculate the shock impedance from the shock velocity data derived from the respective shock Hugoniot to discern the efficacy of dynamic impedance optimization between PUU and glass. New insight on molecular attributes will guide glass/polymer interface designs.

Published by Elsevier Ltd.

1. Introduction

Over the last decade, nature has provided an inspiration towards the rational design of hybrid composites, where hierarchical architectures in structural biological materials such as shells and bones have been correlated with the robust mechanical strength characteristics that were deemed essential for protection against dynamic environmental threats [1–5]. One such concept of note is a gradient approach utilized in the design of graded composites, wherein incorporation of a bone-inspired hierarchy – a soft–-stiff–soft–stiff material distribution pattern based on the bone-foramen and osteonal-bone material systems – demonstrated enhanced shock-wave mitigation capability [4]. Even so, neither nature nor prior experiments did explicitly reveal the role of dynamics at the molecular level. Meanwhile, there is a lack of understanding of the underpinning molecular mechanisms and their influence on material deformation particularly at the moment of impulse interaction. Such knowledge can provide insights towards manipulating the physics of failure for design of robust material systems.

Recently, Veysset et al. used a laser-induced microballistic impact platform and demonstrated its capability of providing real-time, multi-frame imaging for *in-situ* visualization and differentiation of material deformation at strain rates on the order of 10^8/s [6–9]. In particular, the resulting dynamic stiffening phenomenon during such high-velocity impact was first revealed in hierarchical poly (urethane urea), PUU, elastomers but not in a polydimethylsiloxane elastomer, when impacted by silica microparticles [6]. PUUs were noted to exhibit complex microstructure [10–13] along with a broad range of relaxation times [13,14], where the segmental mobility of the soft phase was shown to be strongly dependent upon the extent of intersegment mixing between soft

* Corresponding author. U.S. Army Research Laboratory, RDRL-WMM-G, Aberdeen Proving Ground, MD, 21005-5069, USA.
E-mail address: alex.j.hsieh.civ@mail.mil (A.J. Hsieh).

https://doi.org/10.1016/j.polymer.2018.05.034
0032-3861/Published by Elsevier Ltd.

and hard segments [13–15]. Among these PUUs, soft phases associated with greater phase-mixed regions revealed longer relaxation times on the order of microseconds at ambient conditions [6,13]. The presence of these slower dynamics components were found to be key to enabling dynamic stiffening, presumably via a high-rate deformation-induced glass transition mechanism [7,13], while those with nanosecond relaxation times at ambient conditions were presumably capable of providing additional energy absorption towards dynamic strengthening [6,7]. Furthermore, it was also noted that for PUUs a cooperative molecular relaxation mechanism, facilitated by the presence of intermolecular hydrogen bonding throughout the physically-crosslinked network, could be a plausible pathway towards both dynamic stiffening and dynamic strengthening [7,13,16]. In comparison, PUUs regardless of their respective composition exhibited greater dynamic stiffening during impact at strain rates on the order of 10^8/s than a glassy bisphenol A polycarbonate, despite the high fracture toughness and ballistic strength of the latter [7]. Dynamic stiffening over the same impact velocity range was not evidenced for bisphenol A polycarbonate; instead, plastic deformation was the predominant mode of deformation, presumably due to the lack of a cooperative intermolecular hydrogen-bond relaxation mechanism and a microsecond relaxation [7].

Our motivation for this study is to discern whether the high-rate dynamic stiffening phenomena observed in the bulk PUUs can serve as an effective energy dissipation pathway during ballistic impact at the interface of a glass/polymer bilayer, including the potential of its influence towards shock-wave propagation. Meanwhile, the shock Hugoniot is regarded as the most fundamental description of the thermodynamic state of a material following the passage of a shock wave [17]. Impedance, on the other hand, is a useful concept for better understanding of the flow of impact energy during the ballistic shock events [18,19], where shock-wave impedance differing from the acoustic wave impedance is determined by the product of density and the shock velocity determined at a given impact velocity, hereafter called shock impedance.

In this work, we focus on the molecular influence of polymers where material deformation upon ballistic impact at a glass/polymer interface could be a strong function of their corresponding segmental dynamics. First, we exploit laser-induced microballistic measurements and compare the high strain-rate deformation response of a bulk PUU against impact by silica as well as steel micro-particles, which are of higher impedance than silica microparticles. With respect to the role of segmental dynamics, we utilize broadband dielectric relaxation measurements to further discern and differentiate its influence on the extent of dynamic stiffening observed upon microballistic impact between PUU and a polyurea, PU. In addition, we highlight the essence of high-rate deformation-induced glass transition observed in these bulk elastomers and determine its efficacy towards the dynamic impedance optimization at a glass/polymer interface. This is elucidated through the calculation of shock impedance based on the corresponding shock Hugoniot data.

2. Experimental

The model elastomers chosen for microballistic impact studies and broadband dielectric relaxation spectroscopy measurements included PUU 532–1000 and PU 1000. The PUU 532–1000 was prepared via a two-step, pre-polymer synthesis [20], which is composed of 4,4′-dicyclohexylmethane diisocyanate (HMDI), diethyltoluenediamine (DETA), and poly (tetramethylene oxide) (PTMO), with a molar ratio of 5:3:2 for [HMDI]:[DETA]:[PTMO], where the molecular weight of PTMO is 1000 g/mol. The PU 1000 was formed by reaction of poly (tetramethylene oxide di-*p*-aminobenzoate) (Versalink P1000, Air Products) and a polycarbodiimide-modified diphenylmethane diisocyanate (Isonate 143 L, Dow Chemical) at a 4:1 weight ratio. The molecular weight given by the manufacturer for the PTMO-amine component is $M = 1238 \pm 72$ g/mol. It is noteworthy that the nominal hard segment contents of both PUU 532–1000 and PU 1000 are very similar, ~34 wt.%. More details on the synthesis of PUU and polyurea can be found in Ref. [20] and Ref. [21], respectively, so as on the materials characterization in Refs. [12–15,21–23] as well as in the Supplementary Information section.

The high-strain-rate deformation response of selected elastomers was investigated by using a laser-induced microballistic impact test platform as shown in Fig. 1 [6,24]. The launching pad assembly consists of a 210-μm glass substrate, a 60-nm gold film for laser absorption, a 30-μm layer of cross-linked polyurea (different from the PU 1000), and a sub-monolayer of either silica microspheres (diameter $D = 7.4$ μm) or steel micro-spheres ($D = 20$ μm $\pm$ 2 μm) deposited on top of the assembly as described in Ref. [6]. Upon laser ablation of the gold film using a 10-ns duration, 532-nm wavelength laser pulse focused in a region of about 50-μm diameter, the polyurea layer expands and launches the particles into free space. The particle speed is adjusted from 100 to 800 m/s by varying the laser pulse energy from 2 to 60 mJ (Fig. 1). The projectiles are ejected into free space and impact a target sample at near-normal incidence (±5°). The launching pad and the target are separated by approximately 1.0 mm. Using a high-speed camera (SIMX16, Specialised Imaging), consisting of 16 CCDs, which are independently triggerable, with exposure times as short as 2 ns and variable inter-frame times, we visualized the micro-spheres as they impacted the surface of the samples and subsequently rebounded, providing insight into the high strain rate deformation response of these selected polymeric materials. Both impact and rebound velocities and maximum and residual (final) penetration depths were extracted from the 16-frame videos. The maximum depth of penetration occurs in the first instants following impact; thereafter, the polymer fully responds to the impact and the depth of penetration decreases. A more detailed description of the imaging setup and image analysis is available in Ref. [6].

Dielectric relaxation spectroscopy measurements were carried out using a parallel plate geometry, where samples in the form of disks (15–20 mm diameter, 0.1–0.3 mm thick) were sandwiched between 20 mm diameter brass electrodes to form a parallel plate

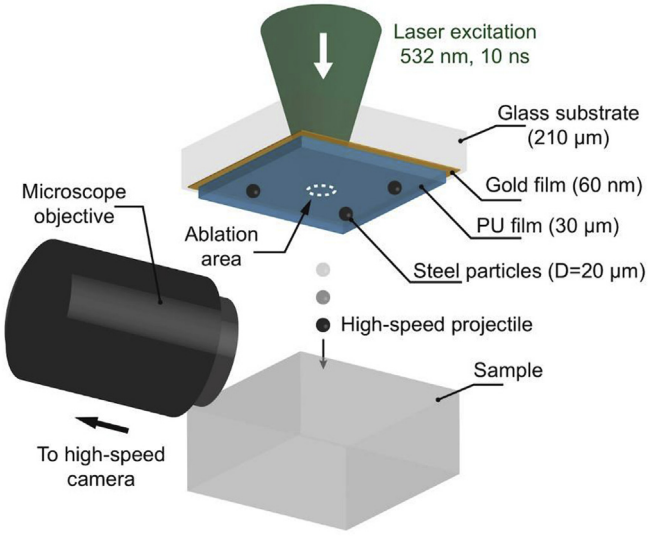

Fig. 1. Schematic of the laser-induced particle impact test.

capacitor. Isothermal relaxation spectra were collected for PUU 532–1000 and PU 1000 under a very dry nitrogen atmosphere as a function of temperature using a Novocontrol Concept 40 spectrometer from 0.01 to 10 MHz on heating from −150 to 200 °C.

3. Results

3.1. Microballistic impact response against silica and steel micro-particles

As shown in Fig. 2, the capability of direct visualization of the impact of micro-projectiles on substrates and *in-situ* characterization, including depth of penetration and the extent of rebound of the micro-projectiles, is clearly demonstrated. In Fig. 2a, representative impact sequences of PUU 532–1000 by silica microspheres of 7-μm diameter are shown, where rebound of a micro-particle is evidenced during impact at 740 m/s, with the sample surface undergoing extreme deformation, at a strain rate on the order of 10^8 s^{-1}, to conform to the impacting spherical projectile. Meanwhile, we also carried out microballistic measurements with 20-μm steel particles to validate our findings on the dynamic stiffening and strengthening characteristics observed in PUUs upon impact by silica micro-particles. Since the steel micro-projectiles are larger and denser than the silica projectiles, it is expected that they would impart greater kinetic energy and momentum. In the case of impact by steel micro-particles, rebound of steel micro-particles still occurs when PUU 532–1000 was impacted at speeds below ~500 m/s. Fig. 2b shows the representative impact sequences observed for PUU 532–1000, where rebound of a steel micro-particle is evidenced during impact at 470 m/s speed. The steel micro-projectile is noted to penetrate to a full diameter under the surface of PUU 532–1000, where the average normalized maximum depth of penetration was found to be greater than those obtained upon impact by silica micro-particles at much higher speeds.

In analysis, we first consider the coefficient of restitution (COR), defined as the ratio of rebound velocity to impact velocity, or the square root of the ratio of the corresponding kinetic energies. The choice of COR is widely used as an empirical parameter to measure the energy dissipation for collisional events involving rebound

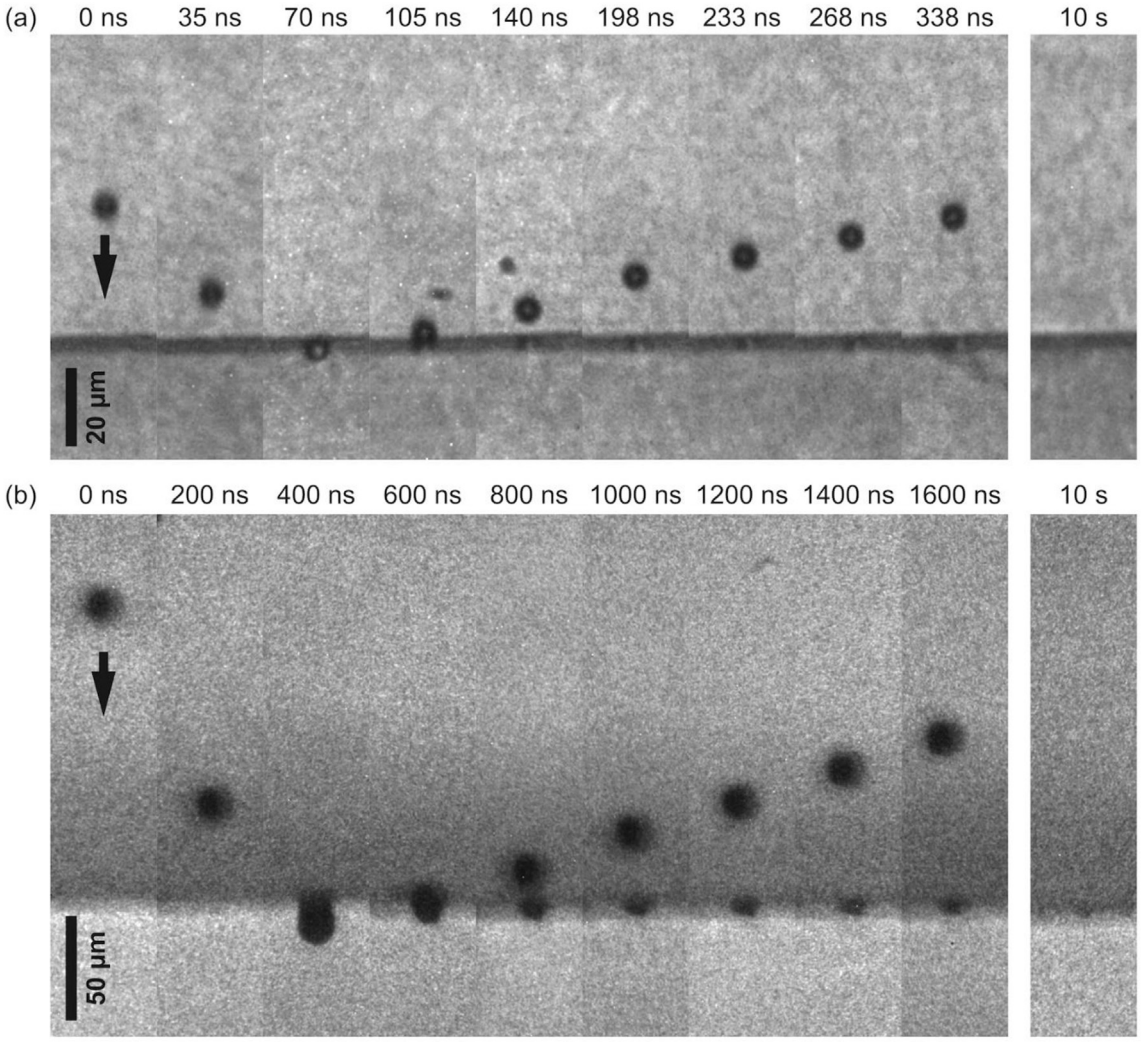

Fig. 2. Typical sequence of images recorded using a high-speed camera with 3-ns exposure time showing particle impact on a PUU 532–1000 sample. (2a) 10 of 16 images of impact by 7.4-μm silica micro-particle with a speed of 740 m/s and (2b) 9 of 16 images of impact by 20-μm steel micro-particle that were recorded in real time by the high-speed camera are presented here cropped from their initial size for the ease of comparison. The time stamps, shown at the top of the frames, indicate the delay in acquisition time relative to the first frame of the sequence. Rebound of micro-particle from the material surface is evidenced in (2a) with a speed of 170 m/s and with minimum penetration as well as in (2b) with a speed of 77 m/s along with maximum depth of penetration of about a full micro-particle diameter.

[25–27]. In Fig. 3a, the COR obtained for the steel and silica particle impacts on PUU 532–1000 are compared as a function of impact velocity. In an ideal case with a completely elastic target the COR would be equal to 1, assuming completely elastic projectiles. Meanwhile, in the case of impact by high-impedance steel micro-particles the resulting impact can drive the target further away from the elastic regime, which results in much lower values of COR, as shown in Fig. 3a. It is noteworthy that as impact velocity reaches a threshold velocity (~500 m/s), complete penetration of steel micro-particles occurs and thereafter, the corresponding COR values become zero. In the case of silica micro-particle impacts, we do not observe such transition even as velocities are increased up to 800 m/s.

In Fig. 3b the COR data obtained for the steel micro-particles impacts on PUU 532–1000 and PU 1000 as a function of impact velocity are compared. As impact speed increases a sudden drop in the COR occurs at around 475 m/s and 400 m/s for PUU 532–1000 and PU 1000, respectively. It is noteworthy that PUU 532–1000 exhibits higher COR over the select impact velocity range as well as higher threshold velocity towards penetration than PU 1000. The compositional influence on the rate-dependent COR is consistent with the corresponding trend observed in the depth of penetration measurements as shown in Fig. 4. A moderate improvement in the resistance against penetration, particularly the normalized residual depth of penetration at higher impact speeds, is noted for PUU 532–1000 over PU 1000, as shown in Fig. 4b. These observations

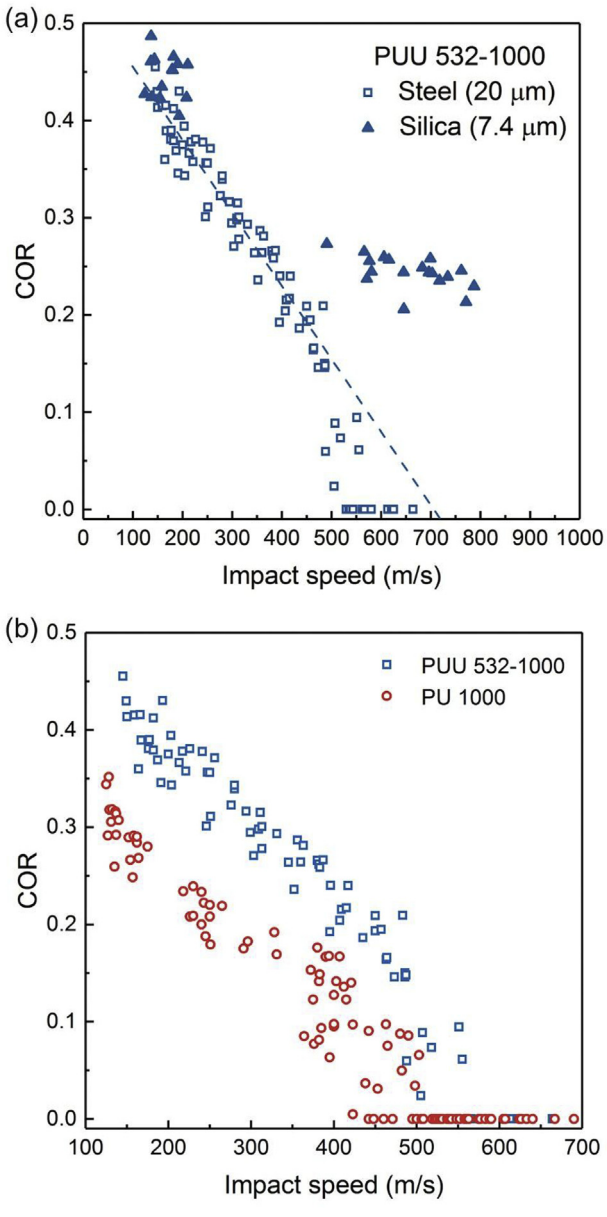

Fig. 3. (A) Comparison of COR vs. impact speed determined for PUU 532–1000 upon impact via 7.4-μm silica particles and 20-μm steel particles. The dashed line represents a linear fit of the data at low speed, 100–400 m/s, evidencing a sudden drop in the COR at around 500 m/s. (b) Comparison of COR data for PUU 532–1000 and PU 1000 impacted with steel micro-particles.

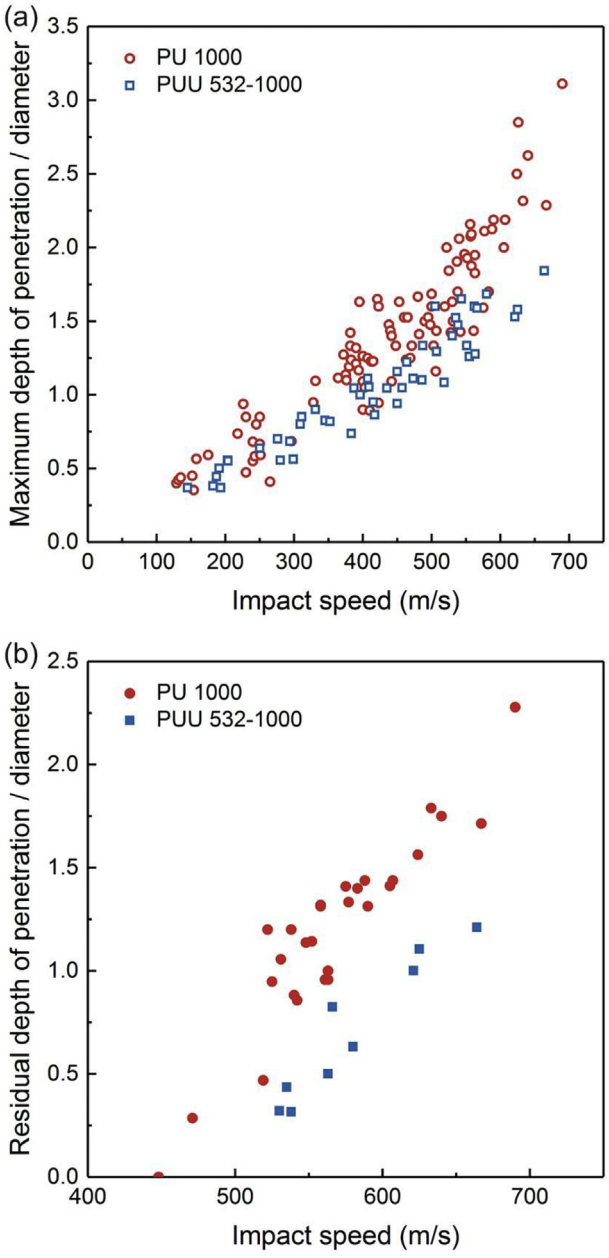

Fig. 4. Comparison of depth of penetration data, including both the normalized maximum depth and normalized residual depth measurements after impact by steel micro-particles, obtained for (a) PUU 532–1000 and (b) PU 1000 as a function of impact speed.

are strongly indicative of greater dynamic stiffening and strengthening characteristics in PUU 532–1000 than PU 1000.

3.2. The molecular influence on segmental relaxation

Herein we investigate the molecular attributes that are of relevance towards dynamic stiffening and strengthening observed upon microballistic impact of the PUU 532–1000 and PU 1000 elastomers. At ambient temperature, the chain segments in the hard domains of both segmented elastomers are immobile [13,21,22]. Thus, we focus on the role of segmental relaxations that are associated with the soft phase of each of the materials and the shift of these relaxations with respect to an increase in frequency, which are determined via broadband dielectric relaxation spectroscopy.

In this work, the broadband dielectric relaxation data are expressed in terms of a derivative form, by taking the logarithmic derivative of the dielectric constant, which has been shown with the same features as the loss spectra but without the dc conduction losses that often obscure low-frequency relaxation processes [28,29]. More details on the broadband dielectric relaxation measurements, including a complete dielectric relaxation spectra as a function of temperature and frequency, obtained for both PUU 532–1000 and PU 1000 are discussed in the Supplementary Information section. In Fig. 5a the isochronal dielectric loss data obtained for both PUU 532–1000 and PU 1000 at 1 Hz are compared. Correspondingly, Fig. 5b reveals the comparison of the dielectric data at 25 °C as a function of frequency. Distinct segmental α and local glassy state β relaxations are clearly evidenced in the PUU 532–1000 data, as shown in Fig. 5b, whereas a very broad ($\alpha_1 + \alpha_2$) process for PU 1000 is observed, in keeping with previous experimental findings [21,30,31]. Both segmental α relaxations are associated with the soft segments in the soft phases of these materials.

In Fig. 5a, a decrease in the dielectric loss, which is associated with the soft-phase segmental α relaxation, is observed for PUU 532–1000 as compared with that of PU 1000, given that both γ relaxations essentially overlap. The γ relaxations are presumably associated with the localized crankshaft motion of the ether oxygen-containing groups in the PTMO soft segments [7,31,33]. The decrease in dielectric loss presumably results from greater intersegment mixing in the soft phase of PUU 532–1000, since the PTMO soft segment molecular weight in each polymer is essentially the same and the corresponding hard segment contents are also similar. In comparison, a decrease in the molecular weight of PTMO [30] or an increase in the wt.% of hard segment [31] also results in a decrease in the dielectric loss observed in the soft-phase α relaxation of polyurea elastomers. Similarly, the influence of composition and microstructure on the extent of loss factor (tan δ) associated with segmental α relaxation of PUUs was also observed in dynamic mechanical analysis (DMA) [22].

In addition, the influence of intersegment mixing is most clearly seen in Fig. 5b in the much lower α relaxation frequency of PUU 532–1000 and in the indicated dynamic glass transition temperatures, −12 °C vs. −36 °C for PUU 532–1000 and PU 1000, respectively, as shown in Fig. 6 (from performing a fit to the Vogel – Fulcher – Tamman (VFT) temperature dependence of the cooperative α process and extrapolating to T_α=100 s). These observations are strongly indicative of the presence of soft phase with much slower segmental dynamics in PUU 532–1000 than in PU 1000. Furthermore, the molecular influence on dielectric relaxation also corroborates well with the corresponding dynamics on the molecular level data determined by the solid-state nuclear magnetic resonance spectroscopy (ssNMR) measurements, where the fraction of rigid-soft-segment component, determined by ^{13}C dipolar dephasing via the time-domain wideline separation (TD-WISE), is much higher than that of PU 1000 (not shown). More detailed information on ssNMR TD-WISE can be found in Refs. [14,15]. Further discussions of the ssNMR data will be reported in a separate publication.

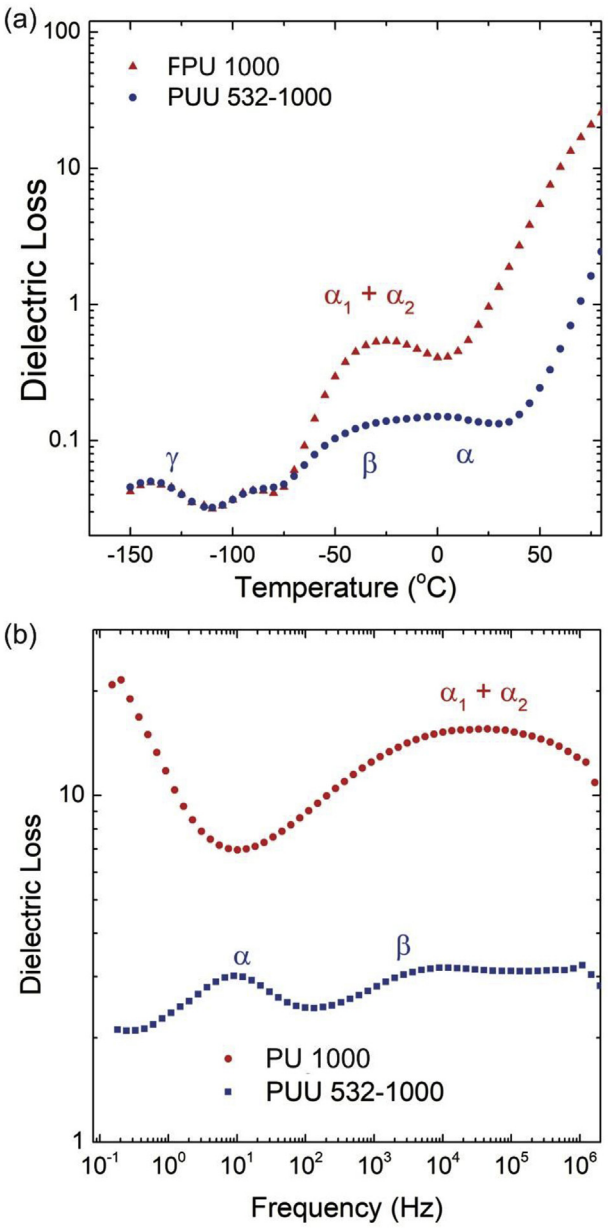

Fig. 5. Comparison of broadband dielectric relaxation data obtained for PUU 532–1000 and PU 1000: (a) isochronal dielectric loss at 1 Hz as a function of temperature, and (b) dielectric loss at 25 °C as a function of frequency.

To highlight the molecular influence, we compared the relaxation frequency maxima vs. the reciprocal temperature data, as shown in Fig. 6. For both PUU 532–1000 and PU 1000, the respective segmental α relaxation reveals the expected VFT temperature dependence nature. Additionally, the segmental relaxation time, τ, was calculated following $\tau = 1/(2\pi f_{max})$, where f_{max} is the frequency of the maximum in the dielectric loss at each temperature [32]. For PUU 532–1000, the τ value of the phase-mixed soft phase at 25 °C is ~1.1×10^{-1}/s, which is about four orders of magnitude slower than that of the broad segmental α relaxation of

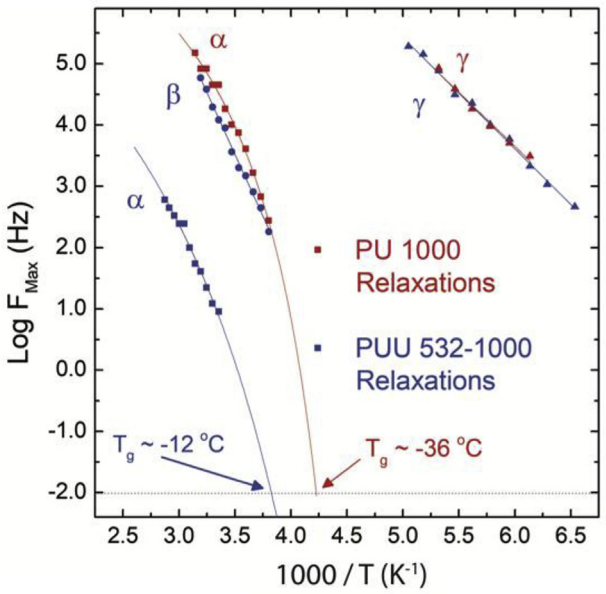

Fig. 6. Comparison of broadband dielectric relaxation data, $\log f_{max}$ vs. 1000/temperature, obtained for PUU 532–1000 and PU 1000, where solid lines are curve-fits of segmental α relaxations to a respective VFT equation (see Supplementary Information section for more details), as well as of β and γ relaxations to a respective Arrhenius equation (see Supplementary Information section for more details). T_gs at $\tau_\alpha = 100$ s were determined to be −12 °C and −36 °C, respectively.

PU 1000, ~2.2×10^{-5}/s. Such differences clearly elucidate that at ambient conditions the PUU 532–1000 would more easily undergo a high-rate deformation-induced glass transition than PU 1000, even when impacted at strain rates on the temporal scale of microseconds. Additionally, for PUU 532–1000 the segmental dynamics of the local β relaxation appears to be very close to that of the segmental α relaxation of PU 1000, indirectly suggesting that the extent of intersegment mixing in PU 1000 is significantly less than that in PUU 532–1000. This difference in the segmental relaxations observed between PUU 532–1000 and PU 1000 is further manifested based on the fact that their respective γ relaxations aforementioned essentially overlap.

Based on these broadband dielectric relaxation data, we expect that PUU532-1000 as well as PU 1000 would undergo high-rate deformation-induced glass transition upon microballistic impact at strain rates on the order of 10^8/s. Meanwhile, PUU 532–1000, having a soft phase with much slower dynamics, would exhibit greater dynamic stiffening, which corroborates very well with the microballistic impact response – higher COR over the select impact velocity range, lower average normalized residual depth of penetration, as well as higher threshold velocity towards penetration, than PU 1000 as shown in Figs. 3 and 4.

4. Discussion

4.1. Molecular influence on shock Hugoniot

The influence of molecular moieties was reported to be increasingly important as impulses become shorter [34]. For the bulk elastomers, both PUU 532–1000 [35] and PU 1000 [36] exhibited similar shock Hugoniot data, which were derived from plate impact measurements, as shown in the Supplementary Information section. Meanwhile, one of the fundamental aspects of shock loading during plate impact is called impedance matching. If two surfaces maintain in contact during impact, the resulting particle velocity, u_p, and stress are presumably the same on both sides of the impact interfaces [37]. Details of plate impact measurements for PUU 532–1000 and PU 1000 can be found in Ref. [35] and Ref. [36], respectively. While PTMO soft segments have the same molecular weight in both polymers, we hypothesize that the presence of strong intermolecular hydrogen bonding in both polymers could also be plausible attributes to the similar shock Hugoniot. For comparison, the shock velocity data obtained for PUU 532–1000 [35] and PU 1000 [36] over the reported impact velocity range are very similar, as shown in Table 1.

4.2. Shock wave propagation at the interface of a glass/polymer bilayer construct

Meanwhile, the nature associated with the refraction phenomenon of a stress wave propagating from one medium to another is known to be complex [18,19]. Here, for simplicity, we consider a one-dimensional steady-state shock wave that reaches the interface between materials of different shock impedance (Z), where the extent of energy that are reflected and transmitted at the interface are known to be dependent upon the difference in Z [18]. The greater the mismatch in Z, the greater the extent of energy will be reflected at the interface.

For illustration, we consider the material response at the interface of a glass/PUU bilayer. For PUU 532–1000, the shock impedance (density × shock velocity) was calculated based on an extrapolation of the available shock velocity U_s data in Table 1 [35], similarly for glass it was calculated based on the reported shock Hugoniot data in Ref. [38]. More details are shown in the Supplementary Information section (Table S2). In brief, there is a significant reduction in the impedance mismatch between the PUU and glass; as u_p increases, the shock impedance for glass is 10.8 MPa-s/m *vs.* 3.2 MPa-s/m for PUU 532–1000 at 0.5 km/s, compared with the respective 11.1 *vs.* 6.6 MPa-s/m at 2 km/s. This is strongly indicative of dynamic stiffening in PUU 532–1000, in spite of having much lower acoustic impedance than glass. Since both elastomers exhibit similar shock velocity data, we envision that PU 1000 is expected to behave very similarly to PUU 532–1000 with respect to dynamic impedance optimization with glass, at the interface of a bi-layer construct, particularly at the moment of impulse interaction.

To highlight the essence of segmental dynamics on dynamic impedance optimization, we compared PUU 532–1000 with glassy bisphenol A polycarbonate. The shock impedance data of PUU 532–1000 are very comparable to those of bisphenol A polycarbonate (see Table S2 in the Supplementary Information section). This is in great contrast to their difference in the corresponding quasi-static properties, such as ambient storage modulus determined via DMA, which is ~0.3 GPa for PUU 532–1000 and much lower than that of polycarbonate, ~1.9 GPa [7]. Thus, unlike metals and glasses, the molecular influence including the enabling high-rate deformation-induced rubber-to-glass transition mechanism can be key to affecting the shock impedance of hierarchical elastomers.

4.3. Influence of microstructure-mediated segmental dynamics on high strain-rate impact response

In addition to considering the shock wave propagation at the interface, the underlying molecular attributes towards dynamic stiffening and strengthening of polymers can be critical to the overall ballistic impact performance of a glass/polymer bilayer. Specifically, we examine the role of segmental dynamics affecting the extent of hyperelastic response observed between these hierarchical elastomers upon impact at strain rates on the order of 10^8

Table 1
Shock Hugoniot data reported for PUU 532–1000 [35] and PU 1000 [36].

	Impact velocity (m/s)	Shock Velocity U_s (km/s)	Particle Velocity u_p (km/s)
PUU 532–1000	298	2.5	0.25
	998	3.6	0.79
PU 1000	279	2.3	0.22
	921	3.5	0.71

s^{-1}. For illustration, we compare the extent of depth of penetration data obtained from the microballistic measurements (Fig. 4a and b) at impact velocities, resulting in similar COR values for PUU 532–1000 and PU 1000. In the case of a COR of 0.25 ± 0.025 (highlighted in Fig. S5 shown in the Supplementary Information section), the respective impact speed was determined to be ~360 ± 60 m/s and ~190 ± 60 m/s for PUU 532–1000 and PU 1000, followed by the corresponding normalized depth of penetration of 0.9 ± 0.2 (Fig. S6) vs. 0.7 ± 0.2 (Fig. S7). These observations reveal that PUU 532–1000 is moderately more hyperelastic than PU 1000 upon microballistic measurements. This is consistent with the aforementioned resistance to penetration data, as shown in Fig. 4, where PUU 532–1000 exhibits moderate improvement in the normalized residual depth of penetration over PU 1000.

Furthermore, we highlight the influence of microstructure-mediated segmental dynamics on dynamic stiffening. For PUU 532–1000, the molecular mobility associated with the β relaxation at ambient temperature is expected to become significantly restricted as the frequency reaches ~10^4 Hz and above, as shown in Fig. 6. Thus, for PUU 532–1000, this local relaxation process would exhibit dynamic stiffening upon microballistic impact at strain rates ~10^8/s. For PUU 532–1000 a shift of the β relaxation temperature to a higher temperature is noted in comparison with that of PUU 211–1000 (not shown). This could be due to the fact that PUUs were synthesized following a pre-polymer route and increasing the molar ratio of the urea vs urethane linkages, from 1:1 for PUU 211–1000 to 1.5 for PUU 532–1000, which could presumably facilitate the ether oxygen containing linkages of soft segments with greater access towards intermolecular hydrogen bonding with ureas. As a result, it is envisioned that a cooperative molecular relaxation that couples soft segments through both segmental α and the local β relaxations could be a plausible pathway for PUU 532–1000 towards dynamic stiffening and strengthening upon impact over the temporal scale of microseconds to nanoseconds.

Although little is known regarding the composition and microstructure of commercially available polyurethane elastomers, we hypothesize that the presence of intermolecular hydrogen bonding readily available in polyurethanes like in PUU and polyurea elastomers could facilitate a cooperative relaxation throughout an interconnected hydrogen-bonded polymer network. This serves as a motivation towards future studies via exploiting atomistic molecular dynamic simulations to further discern and differentiate molecular attributes, including both molecular conformations and intermolecular bonding strength that are of relevance to the dynamic pressure compressibility upon ballistic shock interaction. This would lead to better understanding of molecular mechanisms as well as provide guidance towards design and synthesis of advanced interlayer materials for use in high-performance laminated glass/polymer composites.

5. Conclusion

The influence of molecular attributes that could affect the ballistic shock response at the interface of a glass/polymer bilayer, particularly at the moment of impulse interaction, was investigated.

First, we elucidated the dynamic stiffening characteristics that were observed in PUU elastomers upon microballistic impact by silica micro-particles, which was also evident during impact with steel micro-particles at strain rates ~10^8/s. Rebound of steel micro-particles also occurred when PUU 532–1000 was impacted at speeds below ~500 m/s. Additionally, PUU 532–1000 exhibited higher COR over the select impact velocity range, as well as higher threshold velocity towards penetration, than PU 1000. The compositional influence on the rate-dependent COR is consistent with the corresponding trend observed in the resistance against penetration data. A moderate improvement was noted in the normalized residual depth of penetration data, particularly at higher impact speeds, for PUU 532–1000 in comparison with PU 1000. These are strongly indicative of greater dynamic stiffening and strengthening of PUU 532–1000 than PU 1000. The molecular influence on the extent of dynamic stiffening response corroborated well with the prediction based on the segmental dynamics data determined via broadband dielectric relaxation spectroscopy. PUU 532–1000 exhibits greater intersegment mixing than PU 1000, and as a result T_gs determined at $\tau_\alpha = 100$ s are −12 °C vs. −36 °C, respectively. For PUU 532–1000, the segmental α relaxation associated with the phase-mixed soft phase was determined to be about four orders of magnitude slower than that of the broad segmental α relaxation of PU 1000. Additionally, the segmental dynamics of the local β relaxation of PUU 532–1000 appeared to be very close to that of the segmental α relaxation of PU 1000, which further indirectly suggests greater intersegment mixing in PUU 532–1000 than the latter. We hypothesize that the presence of strong intermolecular hydrogen bonding in both elastomers could be the plausible attributes towards the similar shock Hugoniot data. As a result, it is envisioned that PU 1000 will behave very similarly to PUU 532–1000 when considering the dynamic impedance optimization with glass, at the interface of a bi-layer construct, particularly at the moment of impulse interaction. Meanwhile, PUU 532–1000 is prone to greater dynamic stiffening than PU 1000 upon impact over the temporal scale of microseconds to nanoseconds, presumably due to the presence of well-coupled segmental α and local β relaxations in PUU.

Based on these observations, we hypothesize that a high-rate deformation-induced glass transition mechanism could be a plausible pathway towards dynamic stiffening of hierarchical elastomers, which would otherwise not be realized based on material properties from manufacturers. This is critical, as it could also enable dynamic impedance optimization at the interface between glass and a PUU sub-layer, particularly at the moment of impulse interaction.

Acknowledgments

This material is based upon work supported in part by the U.S. Army Research Laboratory (ARL) and the U. S. Army Research Office through the Institute for Soldier Nanotechnologies, under contract number W911NF-13-D-0001. DV and KAN would also acknowledge support through the Office of Naval Research DURIP Grant No. N00014-13-1-0676. DFM and JR gratefully acknowledge the support of the Office of Naval Research, under grant N00014-14-C-

0205. AJH would like to thank Dr. Robert M. Elder and Dr. John J. La Scala at ARL for fruitful discussions, and also acknowledge Dr. Daniel T. Casem at ARL for the plate impact measurements previously published in Refs. [13] and [34].

Appendix A. Supplementary data

Supplementary data related to this article can be found at https://doi.org/10.1016/j.polymer.2018.05.034.

References

[1] H.D. Espinosa, J.E. Rim, F. Barthelat, M.J. Buehler, Merger of structure and material in nacre and bone – perspectives on de novo biomimetic materials, Prog. Mater. Sci. 54 (2009) 1059–1100.
[2] U.G.K. Wegst, H. Bai, E. Saiz, A.P. Tomsia, R.O. Ritchie, Bioinspired structural materials, Nat. Mater. 14 (1) (2015) 23–36.
[3] Y. Chen, L. Wang, Bio-inspired heterogeneous composites for broadband vibration mitigation, Sci. Rep. 5 (2015) 17865.
[4] J. Huang, H. Durden, M. Chowdhury, Bio-inspired armor protective material systems for ballistic shock mitigation, Mater. Des. 32 (7) (2011) 3702–3710.
[5] M.A. Meyers, P.-Y. Chen, A.Y.-M. Lin, Y. Seki, Biological materials: structure and mechanical properties, Prog. Mater. Sci. 53 (1) (2008) 1–206.
[6] D. Veysset, A.J. Hsieh, S.E. Kooi, A.A. Maznev, K.A. Masser, K.A. Nelson, Dynamics of supersonic microparticle impact on elastomers revealed by real–time multi–frame imaging, Sci. Rep. 6 (2016), 25577, https://doi.org/10.1038/srep25577.
[7] D. Veysset, A.J. Hsieh, S.E. Kooi, K.A. Nelson, Molecular influence in high-strain-rate microparticle impact response of poly(urethane urea) elastomers, Polymer 123 (2017) 30–38.
[8] M. Hassani-Gangaraj, D. Veysset, K.A. Nelson, C.A. Schuh, In-situ observations of single micro-particle impact bonding, Scripta Mater. 145 (2018) 9–13.
[9] M. Hassani-Gangaraj, D. Veysset, K.A. Nelson, C.A. Schuh, Melting can hinder impact-induced adhesion, Phys. Rev. Lett. 119 (2017), 175701.
[10] C.B. Wang, S.L. Cooper, Morphology and properties of segmented polyether polyurethaneureas, Macromolecules 16 (1983) 775–786.
[11] J.P. Sheth, A. Aneja, G.L. Wilkes, E. Yilgor, G.E. Atilla, I. Yilgor, F.L. Beyer, Influence of system variables on the morphological and dynamic mechanical behavior of polydimethylsiloxane based segmented polyurethane and polyurea copolymers: a comparative perspective, Polymer 45 (2004) 6919–6932.
[12] K.E. Strawhecker, A.J. Hsieh, T.L. Chantawansri, Z.I. Kalcioglu, K.J. Van Vliet, Influence of microstructure on micro-/nano-mechanical measurements of select model transparent poly(urethane urea) elastomers, Polymer 54 (2013) 901–908.
[13] A.J. Hsieh, T.L. Chantawansri, W. Hu, K.E. Strawhecker, D.T. Casem, J.K. Eliason, K.A. Nelson, E.M. Parsons, New insight into microstructure-mediated segmental dynamics in select model poly(urethane urea) elastomers, Polymer 55 (2014) 1883–1892, https://doi.org/10.1016/j.polymer.2014.02.037.
[14] W. Hu, A.J. Hsieh, Phase-mixing and molecular dynamics in poly(urethane urea) elastomers by solid-state NMR, Polymer 54 (2013) 6218.
[15] W. Hu, N.V. Patil, A.J. Hsieh, Glass transition of soft segments in phase-mixed poly(urethane urea) elastomers by time-domain 1H and 13C solid-state NMR, Polymer 100 (2016) 149–157.
[16] A.J. Hsieh, T.L. Chantawansri, W. Hu, J. Cain, J.H. Yu, New insight into the influence of molecular dynamics of matrix elastomers on ballistic impact deformation in UHMWPE composites, Polymer 95 (2016) 52–61.
[17] M.A. Meyers, Dynamic Behavior of Materials, John Wiley and Sons, Inc., 1994.
[18] L.F. Henderson, On the refraction of shock waves, J. Fluid Mech. 198 (1989) 365–386.
[19] G.I. Kanel, N.V. Razorenov, V.E. Fortov, The failure waves and spallations in homogeneous brittle materials, in: S.C. Schmidt, R.D. Dick, J.W. Forbes, D.G. Tasker (Eds.), Proceedings of the American Physical Society Topical Conference, Shock Compression of Condensed Matter – 1991, 1991. Williamsburg, Virginia.
[20] S.S. Sarva, A.J. Hsieh, The effect of microstructure on the rate-dependent stress-strain behavior of poly(urethane urea) elastomers, Polymer 50 (13) (2009) 3007–3015.
[21] T. Choi, D. Fragiadakis, C.M. Roland, J. Runt, Microstructure and segmental dynamics of polyurea under uniaxial deformation, Macromolecules 45 (2012) 3581–3589.
[22] R.G. Rinaldi, A.J. Hsieh, M.C. Boyce, Tunable microstructures and mechanical deformation in transparent poly(urethane urea)s, J. Polym. Sci. B: Polym. Phys. 49 (2011) 123–135.
[23] D. Fragiadakis, R. Gamache, R.B. Bogoslovov, C.M. Roland, Segmental dynamics of polyurea: effect of stoichiometry, Polymer 51 (2010) 178–184.
[24] J.-H. Lee, D. Veysset, J.P. Singer, M. Retsch, G. Saini, T. Pezeril, K.A. Nelson, E.L. Thomas, High strain rate deformation of layered nanocomposites, Nat. Commun. 3 (2012) 1164, https://doi.org/10.1038/ncomms2166.
[25] H.H. Calvit, Experiments on rebound of steel balls from blocks of polymer, J. Mech. Phys. Solid. 15 (1967) 141–150, https://doi.org/10.1016/0022-5096(67)90028-2.
[26] G. Constantinides, C.A. Tweedie, D.M. Holbrook, P. Barragan, J.F. Smith, K.J. Van Vliet, Quantifying deformation and energy dissipation of polymeric surfaces under localized impact, Mater. Sci. Eng. A 489 (2008) 403–412.
[27] J. Diani, P. Gilormini, G. Agbobada, Experimental study and numerical simulation of the vertical bounce of a polymer ball over a wide temperature range, J. Mater. Sci. 49 (2014) 2154–2163, https://doi.org/10.1007/s10853-013-7908-2.
[28] M. Wubbenhorst, J. van Turnhout, Analysis of complex dielectric spectra. I. One-dimensional derivative techniques and three-dimensional modeling, J. Non-cryst. Solids 305 (1–3) (2002) 40–49.
[29] J. van Turnhout, M. Wubbenhorst, Analysis of complex dielectric spectra. II: evaluation of the activation energy landscape by differential sampling, J. Non-cryst. Solids 305 (1–3) (2002) 50–58.
[30] A.M. Castagna, A. Pangon, T. Choi, G.P. Dillon, J. Runt, The role of soft segment molecular weight on microphase separation and dynamics of bulk polymerized polyureas, Macromolecules 45 (2012) 8438–8444.
[31] A.M. Castagna, D. Fragiadakis, H.-K. Lee, T. Choi, J. Runt, The role of hard segment content on the molecular dynamics of poly(tetramethylene oxide)-based polyurethane copolymers, Macromolecules 44 (2011) 7831–7836.
[32] C.M. Roland, R. Casalini, Effect of hydrostatic pressure on the viscoelastic response of polyurea, Polymer 48 (2007) 5747–5752, https://doi.org/10.1016/j.polymer.2007.07.017.
[33] D. Fragiadakis, J. Runt, Molecular dynamics of segmented polyurethane copolymers: influence of soft segment composition, Macromolecules 46 (2013) 4184–4190.
[34] N.K. Bourne, On the shock response of polymers to extreme loading, J. Dynamic Behavior Mater. 2 (2016) 33–42.
[35] D.T. Casem, A.J. Hsieh, Plate-impact Measurements of a Select Model Poly(-urethane Urea) Elastomer, Technical Report, U.S. Army Research Laboratory, 2013. ARL-TR-6482.
[36] W. Mock Jr., S. Bartyczak, G. Lee, J. Fedderly, K. Jordan, Dynamic properties of polyurea 1000, AIP Conf. Proc. 1195 (1) (2009) 1241–1244.
[37] W.G. Proud, Notes on Shock Compression, Wave Propagation and Spall Strength, Institute of Shock Physics, Imperial College, London, http://www.mta.ro/wp-content/uploads/2015/12/Proud_William_GSEBS_ImperialCollege_2015_-4.pdf.
[38] W. Carter, S. Marsh, Hugoniot Equation of State of Polymers, Technical Report LA- 13006-MS, Los Alamos National Laboratory, 1985.